INTERNATIONAL JOURNAL OF BIOLOGY AND BIOMEDICAL ENGINEERING
DOI: 10.46300/91011.2022.16.4 Volume 16, 2022

A Functional Electrical Stimulator to Enable Grasping Through Wrist Flexion

Mahendra S. J.[1], Viswanath Talasila[2], Abhilash G. Dutt[3], Mukund Balaji[3], Abhishek C. Mouli[3]
[1]Research scholar, VTU Belagavi, Department of Medical Electronics Engineering, M S Ramaiah Institute of Technology Bangalore, Karnataka, India. [1]mahendra.j@msrit.edu
[2]Department of Electronics and Telecommunication Engineering, Center for Imaging Technology, M S Ramaiah Institute of Technology Bangalore, Karnataka, India. [2]viswanath.talasila@msrit.edu
[3]Department of Medical Electronics Engineering,M S Ramaiah Institute of Technology Bangalore, Karnataka, India. [3]abhilashgdutt@gmail.com

Received: June 7, 2021. Revised: November 16, 2021. Accepted: December 10, 2021. Published: January 3, 2022.

Abstract- Functional electrical stimulation is an assistive technique that utilizes electrical discharges to produce functional movements in patients suffering from neurological impairments. In this work, a biphasic, programmable current- controlled functional electrical stimulator system is designed to enable hand grasping facilitated by wrist flexion. The developed system utilizes an operational amplifier based current source and is supported by a user interface to adjust stimulation parameters. The device is integrated with an accelerometer to measure the degree of stimulated movement. The system is validated, firstly, on two passive electrical loads and subsequently on four healthy volunteers. The device is designed to deliver currents between 0-30mA, and the error between the measured current and simulated current for two loads were -0.967±0.676mA and -0.995±0.97mA. The angular data from the accelerometer provided information regarding variations in movement between the subjects. The architecture of the proposed system is such that it can, in principle, automatically adjust the parameters of simulation to induce the desired movement optimally by measuring a stimulated movement artifact (e.g., angular position) in real time.

Keywords- Function Electrical Stimulation, Programmable Stimulator, Wrist Flexion, Grasping

I. INTRODUCTION

Across the globe, an estimated 2.5 million people are affected by spinal cord injury (1), and about 33 million people are affected by stroke, with the majority of cases reported in low and middle-income countries (2). Severe impediment of voluntary motor control is a feature of stroke and spinal cord injuries. The functional loss of the utility of limbs is a consequence of the secondary process post the disruption of the neuron's standard structure and its network after the injury (3). The loss of voluntary motion control affects the ability to perform everyday activities and negatively impacts an individual's quality of life. As a consequence of long-term care, the affected individuals experience tremendous social and economic challenges.

Functional electrical stimulation is a neuro-rehabilitative intervention based on the application of electrical pulses to an actuating muscle group to generate functional muscle contractions (4) in patients with impairments due to stroke or spinal cord injury. Muscle activation due to FES is characterized by synchronous activation of muscle groups (5) and quick activation of fast-twitch fibers over slow-twitch fibers (6). For functional electrical stimulation to be successful, the motor neurons, muscle tissues, and neuromuscular junctions must be healthy (6).

Several prostheses have been designed using FES for various applications to promote and restore voluntary motor function after an injury. Intervention through FES emphasizes on improving strength, range of motion and stability. FES can be used to rehabilitate both upper and lower limbs. Lower limb rehabilitation focuses on gait (7), prevention of foot drop while walking, and restoration of the ability to sit, stand and walk (8). In contrast upper limb rehabilitation focuses on restoring the functional ability of the arms (9) to complete activities such as bathing, drinking, and eating (10). Rehabilitation focusing on recovering the ability to grip and grasp is vital to perform these activities. In this work the hand grasping movement enabled by wrist flexion is considered.

Existing clinical FES systems are primarily based on circuits that utilize transformer and MOSFET architectures. These designs generally have a large component count and are bulky (11). On the other hand, designs based on operational amplifiers have the advantages of flexible and efficient design without large components, but they have not been validated in clinical scenarios (12). Furthermore, the response evoked by standard functional electrical stimulator systems based on the considerations explained in Section 2.2 is nonlinear and dynamic (13). Existing systems cannot adjust the parameters of stimulation to compensate for unpredictable effects like fatigue, variation in response to change in electrode positioning, voluntary contribution to the movement, and level of spasticity (14). The current solution to this problem is to introduce stimulation with large intensity to generate exaggerated muscular responses to compensate for these effects at the cost of early onset of muscle fatigue (15). Therefore, there is a need for solutions that can effectively tackle this issue. The use of external sensors to capture movement and

muscle contraction dynamics allows for assessing the effects mentioned above and compensating for the same. Integration of motion (16) and EMG sensors (17) with the stimulation unit enables the collection of vital information of human motion and muscle contraction. The information gathered supports the development of control strategies (18) to overcome the mentioned challenges.

Therefore, this work aims to design, test, and validate a biphasic programmable electrical stimulator system that can enable hand grasping and continuously measure the degree of stimulated movement in real-time. The developed device is characterized by performing circuit simulations and experimental tests on resistive loads. Subsequently, to validate the effectiveness of the device to facilitate the grasping motion, an experiment was conducted on healthy human subjects where the response to the electrical stimulation was captured using an accelerometer.

In Section 2 of this work, the primary components of a standard FES system are described along with the essential technical and clinical considerations that must be taken into account while designing FES systems. Section 3 presents the development of an FES system to enable hand grasping. This section also provides information regarding the experimental setups and approach. In Section 4, the characteristics of the device and results of the experiments conducted on passive electrical loads and healthy human participants are reported. The findings and limitations of this work are discussed in detail in Section 5 before concluding this work in Section 6.

II. COMPONENTS AND DESIGN CONSIDERATIONS OF AN FES SYSTEM

A. *Components of an FES system*

An FES device comprises of an electrical stimulator component capable of delivering the electrical pulses for stimulation and a pair of electrodes to deliver the pulses to the tissues.

Electrical Stimulator: The electrical stimulator is responsible for generating the electrical pulses. The generated pulses can be either voltage regulated or current regulated, as discussed in Section 2.2. The electrical stimulator may employ several waveforms for stimulation. The monophasic pulse, biphasic pulse, and exponential pulses have been considered in numerous research settings (19). Figure 1a & 1b illustrate the monophasic and biphasic pulses, respectively. Furthermore, a charge-balanced biphasic stimulation pulse with an interphase delay is also generally considered and illustrated in Figure 1c. The advantages and limitations of these pulses are discussed in Section 2.2. The electrical stimulators may also employ either one or multiple channels to deliver the pulses. A multi-channel system with switch settings allows the delivery of the stimulation to different muscle
groups.

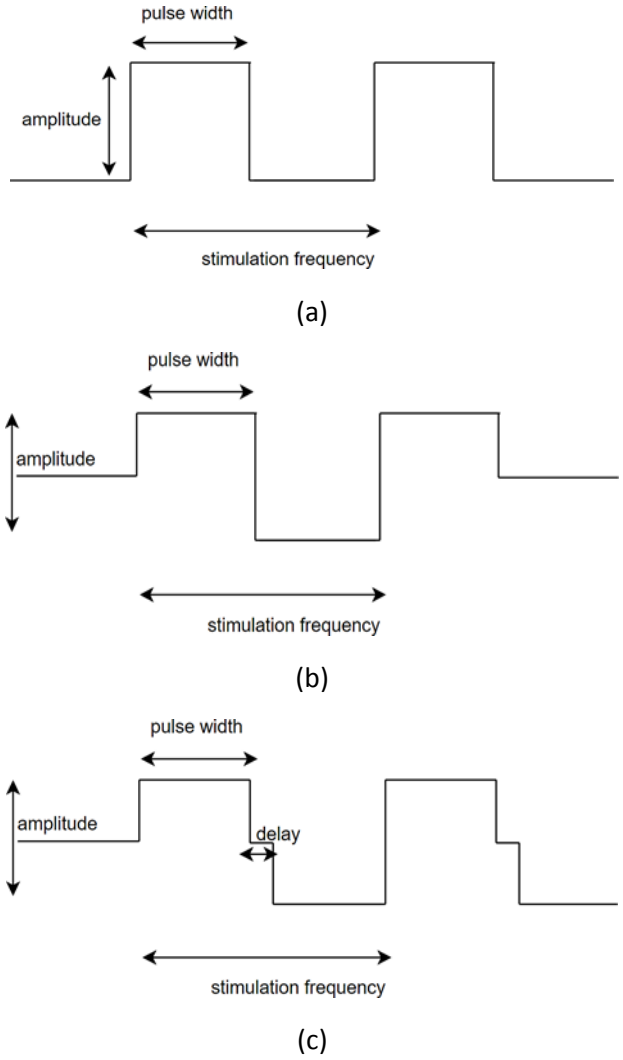

Fig. 1 Various rectangular pulses used for functional electrical stimulation. a) monophasicpulse b) Biphasic charge balanced pulse c) Biphasic charge balanced pulse with interphase delay

Electrodes: Electrodes form the interface between the stimulating device and the tissue. Stimulation can be delivered to the target tissue using surface(transcutaneous), percutaneous, or implantable electrodes. The former two being minimally invasive and invasive, respectively, are not considered in this work. On the other hand, transcutaneous electrodes are non-invasive and are placed on the surface of the body. Generally, the electrodes are self-adhesive and are pre-gelled to reduce the electrical impedance at the point of contact. The drawback of these electrodes is that deep underlying muscle groups are not easily accessible. As a result, a pulse of larger intensity is required to obtain a response, which in turn also excites undesired muscles (20).

B. *Design considerations of an FES system*

Before designing an FES system, it is essential to consider attributes related to the technical, practical, and clinical aspects of the device. The characteristics of the pulse-like the shape, intensity, duration, and frequency, are some

technical aspects, while the placement of the electrodes for stimulation and the effects of stimulation on tissues are the practical and clinical aspects of FES.

- **Voltage and Current Controlled Stimulation:** The stimulus injected to excite the cells can take the form of voltage or current pulses. In voltage-controlled stimulation, the current flowing through the tissue cannot be precisely controlled as the current depends on the impedance at the electrode-tissue interface. In current-controlled stimulation, the current flowing through the tissue can be precisely controlled (21). Therefore, current controlled stimulation is preferred over the former.

- **Pulse Amplitude, Duration and Frequency:** The characteristics of a stimulus pulse apart from the type of waveform used is described by its amplitude, duration, and frequency. The degree of motion produced by a muscle in response to electrical stimulation can be regulated by varying the amplitude, pulse duration/width, and frequency of the stimulating current. The stimulation amplitude corresponds to the magnitude of the delivered current. It directly affects the degree of contraction. Large stimulation intensities invoke stronger contraction in muscles (22). The relationship between muscular activity and pulse amplitude is described in (23). The pulse duration/width is the duration for which an electrical pulse is present. Long pulse duration requires a small amount of current to generate a response, while short pulse duration requires a more considerable amount of current to generate a similar response (24). The relation between duration against the degree of nerve recruitment during transcutaneous electrical stimulation is illustrated in Figure 2. The recruitment follows Equation 1 (25), where rec_{sat} is the value where recruitment saturates, τ is the time constant of rising recruitment, and PD0 is threshold pulse duration, such that rec = 0, for PD < PD0.

$$rec = rec_{sat} * [1 - e^{(-(PD-PD0)/\tau)}] \quad (1)$$

The stimulation frequency, on the other hand, controls the delivery rate of the electrical pulses. High-frequency stimulation triggers additional muscle contractions (before the muscle relaxes) compared to low-frequency stimulation (26). Multiple prolonged contractions induce a sustained force where no single contraction is observed.

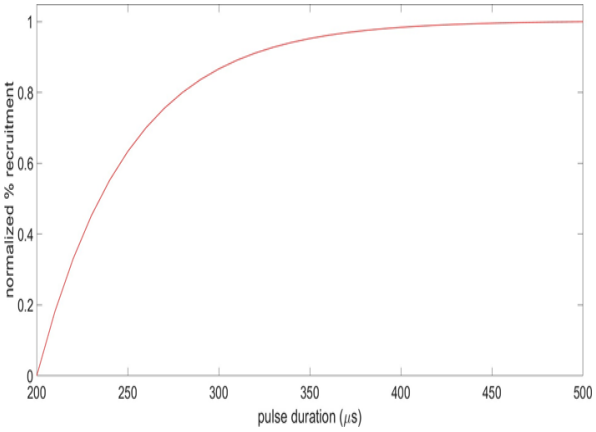

Fig. 2 Illustration of a typical muscle

recruitment curve depending on pulse width for a Constant amplitude (25).

- **Stimulation Waveform Type and Shape:** The stimulation waveforms used for FES can be rectangular or non-rectangular. Non-rectangular pulses such as exponential, sinusoidal, and Gaussian have been previously implemented in research settings. Although they offer advantages over rectangular pulses (27), they are not pursued further in this work. The rectangular pulses used for FES can be broadly classified as monophasic and biphasic waveforms. When monophasic pulses are used for stimulation, the current only flows in one direction between the electrodes. It is documented that upon prolonged stimulation, the electrode potential gradually drifts towards more negative values. This effect has two implications. Firstly, the efficacy of the stimulation increases as currents with smaller amplitudes are sufficient to trigger the tissues (28). Secondly, due to the negative electrode potential, several electrochemical reactions (29) occur at the interface, which is harmful to the tissues. On the other hand, when biphasic pulses are used, the current flow is bi-directional, and the second phase of the pulse is used to reverse the electrochemical reactions at the interface (29). Therefore, the harmful effects of the reactions at the interface can be avoided. A charge balanced biphasic pulse, however, has the tendency to subdue tissue responses, which would otherwise normally be observed with monophasic stimulation. Therefore, an interphase delay is introduced between the positive and negative phases in order to restore the response threshold (28). Figure 1(a), (b), and (c) illustrates typical monophasic, biphasic, and biphasic pulse with interphase delay waveforms.

- **Placement of Electrodes:** The placement of the working and return electrodes impacts the type of muscle contracted. It is essential to identify optimal electrode positions for an individual (30) and utilize small sized electrodes (31) to stimulate a specific group of muscles without unwanted co-activation. For instance, Figure 3 shows the ideal position of the electrodes for wrist flexion and grasping action.

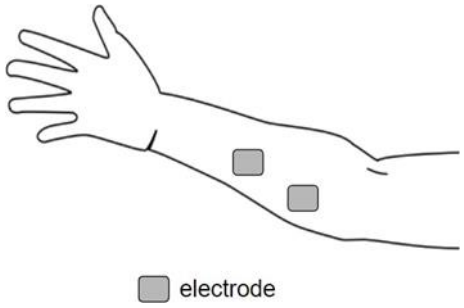

Fig. 3 Optimal electrode placement determines the group of muscles activated. The figure illustrates the placement of electrodes for enabling the grasping action induced by flexion. The negative electrode is placed slightly higher to the medial condyle and between the wrist and finger flexor. The positive electrode is placed over the flexor surface of tendons on the forearm (32).

- **Electrode-Skin Interface:** The nature of the electrode-skin interface determines the effectiveness of the current delivered during FES. The electrode skin interface can be decomposed into the electrode-electrolyte interface and the electrolyte-skin interface. Figure 4 illustrates the electrode-electrolyte interface. Charges distributed locally across the electrode-electrolyte interface correspond to a capacitive double layer (Cd), which creates a potential difference across the electrode-electrolyte interface, known as half-cell potential (Vh) (33). The resistance offered to the flow of charges through the double layer, and the electrolyte are represented by Rp and Rs in Figure 4, respectively. The skin-electrolyte interface is illustrated in Figure 4. The layers of the skin (epidermis, dermis and subcutaneous) are electrically modelled as parallel RC components. Stimulated current flows between the electrodes through the electrolyte. The current flows through the epidermis by - (a) lipid-corneocyte matrix pathway and (b) appendageal pathway (34). Structural variations at the interface and electroporation of the skin change the electrical properties at the interface (35).

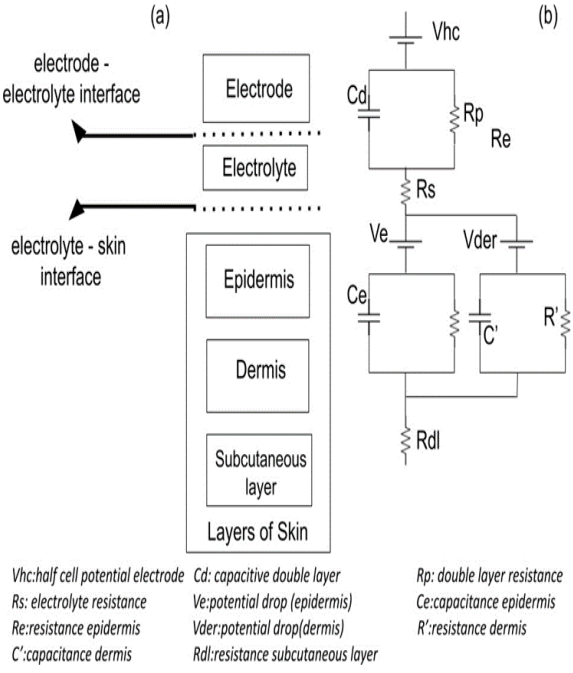

Fig. 4 Illustration of the electrode-electrolyte- skin interface. (a) The electrode- electrolyte-skin interface. The skin is represented by three layers - epidermis, dermis and the subcutaneous layers (33). (b) The equivalent model of the electrode-electrolyte-interface.

- **Clinical Considerations:** There are several clinical considerations for the use of electrical stimulation to artificial actuate muscles. Some considerations are the maximum current intensity, skin injuries and irritation due to electrodes (36), effect of stimulation on subjects with thick subcutaneous layers (37), and interaction of the stimulator with other wearable devices (pacemakers, Holter monitors) (38).

Figure 5 illustrates the system level block diagram of the developed system. The main subsystems of this device include a power system module, microcontroller unit, output driving module, data logging unit through serial interface, and an external motion sensor.

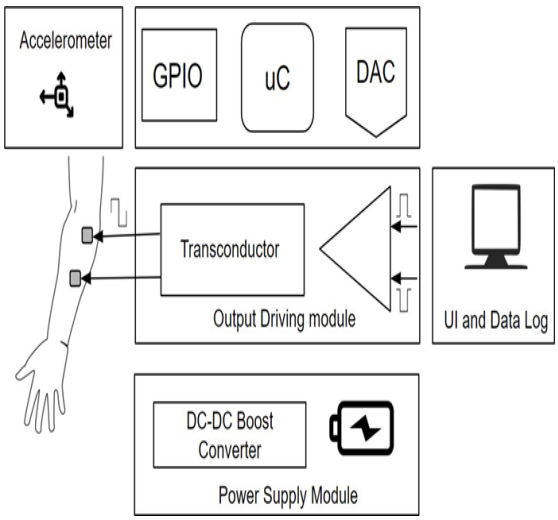

Fig. 5 Block diagram of the programmable functional electrical stimulator system

Power system module

A 9V 600mAh (Hi-Watt) battery was used to sustain the power requirements of the system. The XL6009 DC-DC boost converter was used to step up the voltage to a desired level of ±16V. The boosted voltage is utilized for the rail-rail supply for the output driving stage. A dedicated 3.3V LDO is used to power the microcontroller unit.

Processing unit

The processing unit of the device is based on the STM32F446 (STMicroelectronics), featuring a 32-bit cortex M4 core. The unit facilitates the generation of pulse trains, acquiring the data from the accelerometer, and transmit and receive serial data from a user interface. The microcontroller is programmed to operate in two modes, as shown in Figure 6. In the first idle mode, no peripheral functions are performed, and the device is idle. In the second mode, the peripheral functions are executed as

required by the user. The microcontroller is configured to generate two independent uniphasic pulse trains with varying amplitude and duration using the internal digital to analog converter. The individual pulses are fed to the input of the driving modules. Furthermore, the microcontroller is configured to obtain the data from the accelerometer through the I2C interface.

Output driver module

The output driving module primarily consists of a difference amplifier and an improved Howland current source as the voltage to current converter. The difference amplifier segment of the output driving module is utilized to convert the two single uniphasic signals from the microcontroller DAC to a single biphasic wave.

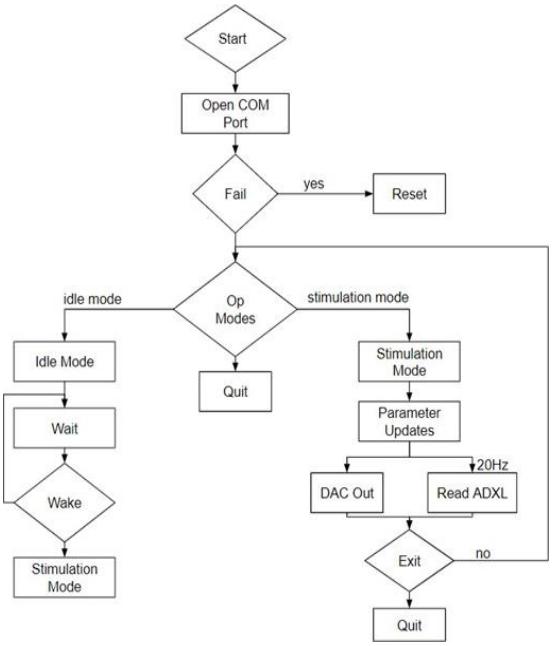

Fig. 6 Illustration, represents the flow of operation of the device.

The uniphasic signals between 0 and 3.3V is mapped to a biphasic signal between 0-250mV. The output of the difference amplifier is supplied to the input of transconductor stage (Howland Topology). Figure **7** illustrates the incorporated Howland circuit. A two operational amplifier topology is used where a buffer (A1) is inserted into the inverting terminal of the amplifier A2 to improve the output impedance of the system. The advantage of the circuit is its superior current drive capability (39). In Figure **7**, if the resistor ratio (R1/R2) equals (R3/R4+Ro), then the current at the output is only dependent on the input voltage Vi and Ro and independent of the load. This is however an ideal scenario. Resistor tolerance and mismatches are known to affect the precision of the current delivered at the output (40).

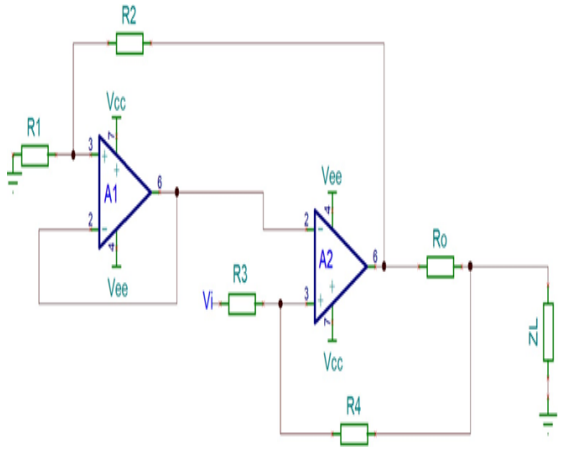

Fig. 7 Schematic of the output driving module. With the use of well-balanced resistors, the current through the load is dependent on Vi and Ro

Data logging and user interface

A user interface (hosted on a computer) designed using Python allows the user to communicate with the microcontroller. The user interface allows the user to switch between operation modes and commands the microcontroller to transmit the data acquired from the accelerometer through a serial interface for storage.

Motion sensor

An ADXL345 digital accelerometer was used to measure the linear acceleration with respect to positional changes. The accelerometer was configured to measure with a 2g range and 12-bit resolution. The data was sampled at 20Hz, and the raw 12-bit signal was converted to the g value.

III. EXPERIMENTAL SETUP AND PROTOCOL

The objectives of the experiments were to assess (a) accuracy of the current delivered by device with respect to the simulated outputs (as described in A), (b) characterize the digital to analog converter, (c) assess the ability to measure the movement induced time- locked with stimulation, and (d) demonstrate the ability of the current injected by the device to enable hand grasping task facilitated by flexion of the wrist.

A. Experiment 1: Testing the device on resistive loads

To assess the accuracy of the current delivered by the device with respect to the simulated outputs, the device was tested against two resistive loads (220Ω and 330Ω). The selection of loads is based on estimated forearm impedance values at theoretical low frequencies derived from the Cole-Cole plot (41 42,43,44). Nine DAC values (corresponding to current levels between 4 - 30mA) were programmed through the user interface, and the current through the loads was measured. The error of the output current with respect to the simulated current was determined.

B. Experiment 2: To Demonstrate the ability to facilitate hand grasp Participants

Four healthy volunteers (three males and one female, aged between 22-58 years) were recruited for the experiments after informed consent. Table 1 lists the information of the four subjects recruited for the study. The subjects are identified in this work as S1, S2, S3, and S4. The inclusion criteria were: age older than 18 years, sufficient proximal arm function, no skin allergies, no metallic or electrical implants, not pregnant, and no known cardiovascular condition.

Table 1 Information of the Subjects Recruited for the Study

Subject	Age	Sex	Height (cm)	Weight (Kg)	BMI (kg/m2)
S1	24	Male	180	70	21.6
S2	22	Male	180	66	20.3
S3	58	Male	162	65	24.8
S4	53	Female	157	72	29.2

Experimental process

Before starting the experiment, general anthropometric data such as age, height, and weight were collected. Subsequently, electrodes and accelerometers are placed on the body. The electrodes (Physio Future International, Dimension: 5cm x 5cm) were placed on the right forearm, as shown in Figure3 after cleaning the surface of the skin. Each participant was made to sit comfortably with their arms resting on the table and supported against gravity without any constraints or contraptions. An accelerometer was placed on the dorsal region of the palm using a velcro band to faithfully capture the grasping motion. For all participants, the stimulation was delivered at the electrode site using biphasic current pulse trains with a train duration of 7s. The pulse frequency was set to 50Hz. During the experiment, the pulse duration and stimulation intensity were varied. A combination of four pulse duration (200μs, 220μs, 240μs, and 260μs) and five stimulation intensities (19.04mA, 21.76mA, 23.12mA, 25.84mA, and 27.2mA) were chosen as variable parameters. The current intensities are determined based on five digital to analog count levels - 2800, 3200, 3400, 3800 and 4000. If a participant experienced muscle fatigue or pain, the stimulation was turned off instantly.

Data analysis

The data recorded were exported and analyzed using MATLAB (R2020b, MathWorks Inc). The raw accelerometer data were filtered using a median filter to remove spike- based artifacts. The grasping angle (along the flexion-extension axis) was calculated using Equation 2, and the roll angle (along the longitudinal axis of the forearm) was calculated using Equation 3.

$$\theta = \arccos\left(z_g / \left(x^2{}_g + y^2{}_g + z^2{}_g\right)^{1/2}\right) \quad (2)$$

$$\varphi = \arctan\left(y_g / z_g\right) \quad (3)$$

IV RESULTS

A. Device characteristics

Table 1 describes the simulated characteristics of the device. Figure 8 illustrates the simulation of a stimulation protocol where the pulse duration is 200μs, and frequency is 50Hz. The rise time and settling time of the circuit is 7.26μs and 19.10μs, as illustrated in Figure 9. Simulations revealed that for RC load combination (R varying from 200Ω to 1kΩ and C varying from 8μF to 12μF), the -3dB frequency (current magnitude vs. frequency) is at 80kHz.

Table 2 Simulated Device Characteristics

Features	Desription
Amplitude (programmable)	0-30mA
Frequency Range (programmable)	20-5kHz
Pulse Width, Duty Cycle	200 - 1000μs (programmable duty cycle)
Settling Time	19.10μs (0 - 3.3V step input)
Rise Time	7.26μs (0 - 3.3V step input)
-3db Freq (Current Magnitude vs Frequency)	80kHz for RC load combination (R varying from 200 Ωto 1kΩ and C varying from 8μ F to 12μ F)

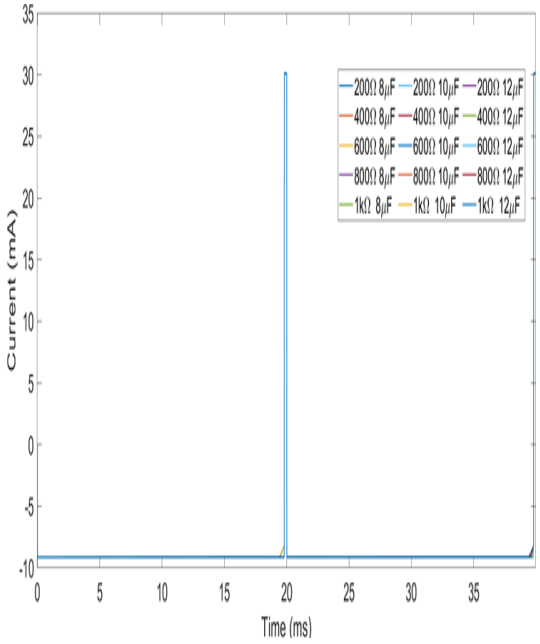

Fig. 8 Output biphasic current pulse wave for various load combinations for a 3.3V input. The pulse duration of the positive half is 200μs.

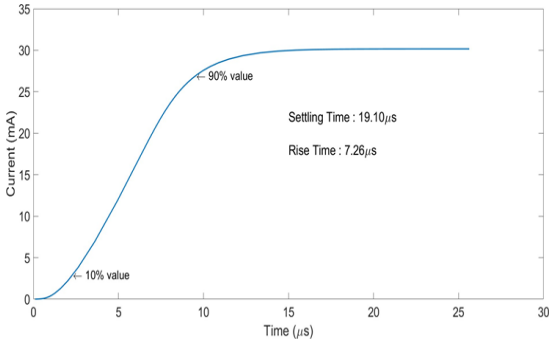

Fig. 9 Output of the system for a 3.3V step input. The rise time is 7.26μs and settling time is 19.10μs.

B. Testing the device on resistive loads

Figures 10a and 10b illustrate the measured current values against the programmed current values for Loads 1 and 2 respectively. The correlation between the measured and programmed current values is high (Load 1: r=0.997 and Load 2: r=0.994). The error (mean±SD) between the current values is -0.976±0.676mA for load 1 and –0.995±0.97mA. The error between the loads was 0.018mA±0.9104mA. Figure 11 illustrates the linear input-output relationship between the digital to analog converter count and the measured output current. The simulated and experimentally determined sensitivities are 0.0073mA/DAC count and 0.0068mA/DAC count respectively.

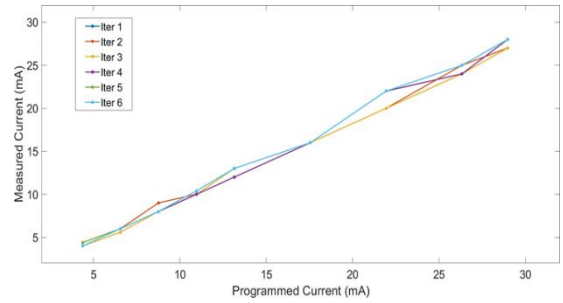

(a)

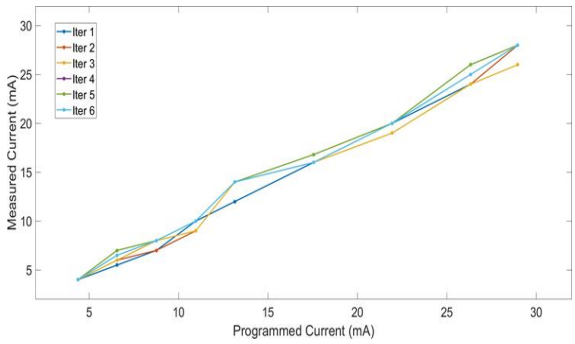

(b)

Fig. 10 A close relationship between the measured and programmed current was observed for (a) Load 1 - 220Ω and (b) Load 2 - 330Ω.

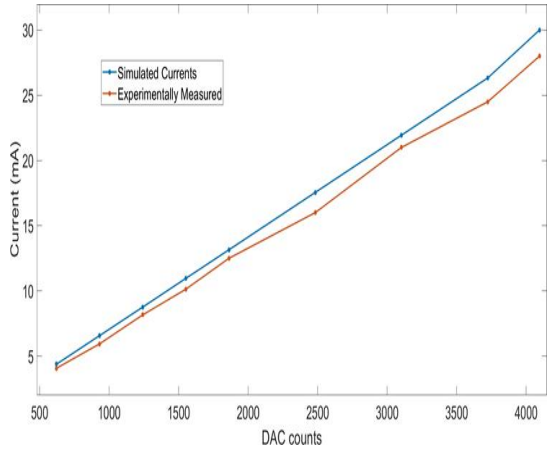

Fig. 11 Input - output characteristics of the system. The relationship was linear. Figure illustrates the relation between the stimulation current injected in response to a range of voltages sent out by the microcontroller's digital to analog converter.

C. C Testing the device with subjects

Figure 12 represents the continuous measurement of the grasping angle for a particular protocol stimulus (pulse width = 240 and I = 23.12mA) for a sweep time of 7s. From the figure, it can be seen that the movement of the wrist saturates after a gradual rise period. Additionally, it is observed that the range of movement is unique for each subject. While S1 and S3 show a large range of motion, S4 and S2 hardly show any considerable movement from the resting position. It is also interesting to note that the time taken to reach the saturation level also varies greatly.

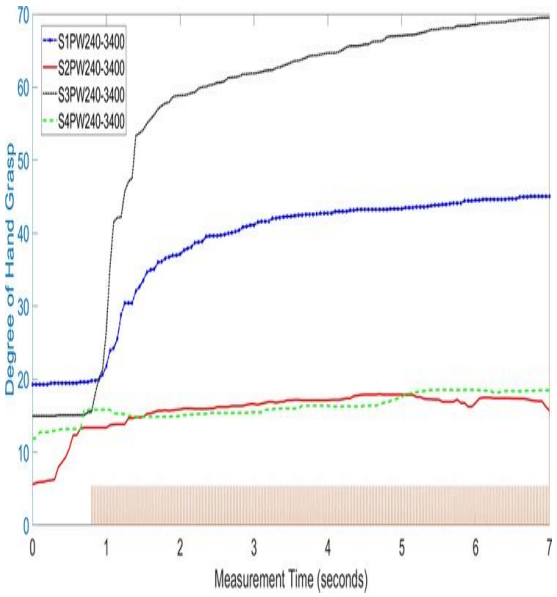

Fig. 12 Continuous measurement of the grasp angle and corresponding stimulation pulse train (normalized in this illustration) with pulse width: 240, DAC level: 3400 (23.12mA).

Figures 13a-d represents the mean angle (grasping) measured after saturation for varying current levels and pulse duration. S1 showed the most extensive range of motion (107◦) and S4 showed the smallest range (30◦) at 27.2mA and pulse width = 220µs. As a general trend, it

was observed that as the current levels increased, the magnitude of motion also increased. Except for S4, the response to stimulation beyond 21.76mA was quite significant. S4 showed considerable motion only after 25.84mA. It was also observed for S2, that the degree of grasp observed with pulse widths = 200µs and 220µs at 19.04mA and 21.76mA was more significant than for pulse widths = 240µs and 260µs. An unusually large variation in the measurement of angles was observed for S1 for pulse widths = 220µs and 200µs at current amplitude 25.84mA. Furthermore, from the data, it was interesting to note that a consistent trend between the degree of motion and pulse width (while keeping the pulse amplitude constant) was not observed for any of the subjects.

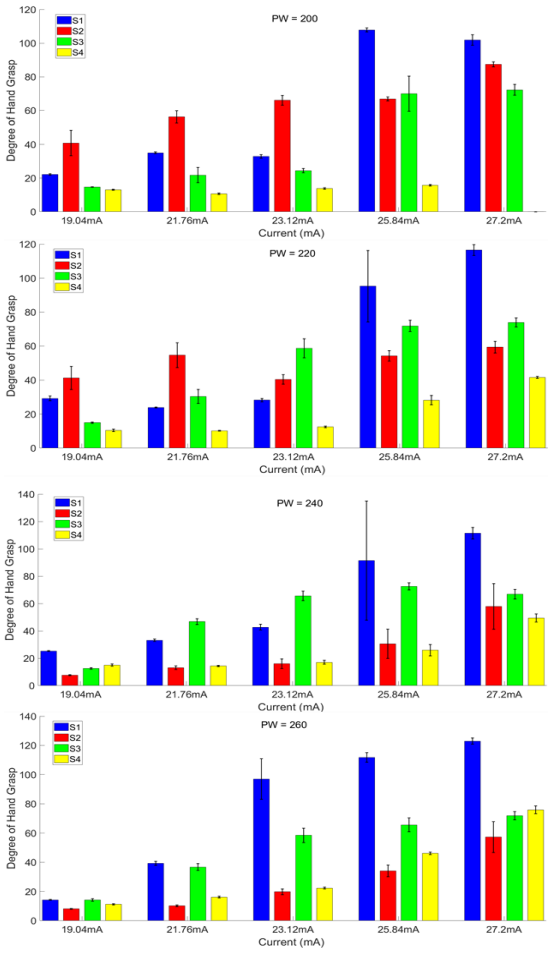

Fig. 13 Mean degree of movement (grasp) in response to the stimulus intensity for S1-4. (a) pulse width (PW) = 200, (b) 220, (c) 240 & (d) 260 (note: For S4, data was not collected for PW=200 and I=27.2mA)

During the experiment, apart from the movement about the flexion-extension axis, a rolling motion was also observed about the longitudinal axis of the forearm. Figures 14a- d illustrate the mean degree of roll. Except for S1, the rolling motion observed for other subjects was in the negative direction. For S1, the rolling motion was in the negative direction for stimulation amplitude less than 25.84mA (except pulse width = 260µs at 23.12mA), exceeding which would cause a rolling motion in the positive direction. Additionally, a positive rolling motion was observed for S2 for amplitudes 23.12mA and 25.8mA at pulse width = 200µs. Maximum rolling in the negative direction was observed for S4 (-69.59◦ for PW = 260µs, I = 27.2mA), and maximum rolling in the positive direction was observed for S1 (76.836◦for PW = 200µs, I = 27.2mA).

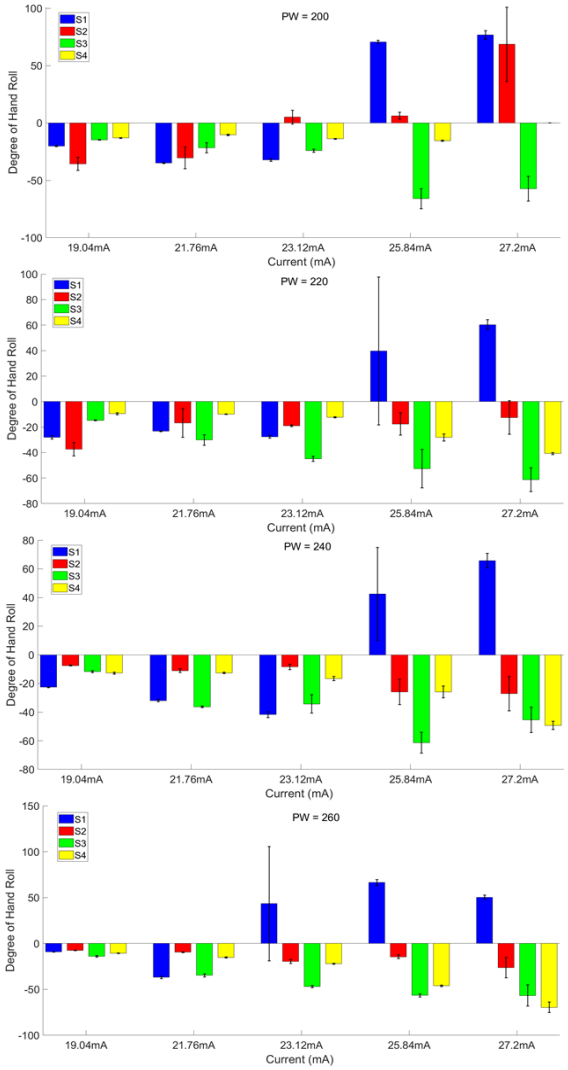

Fig. 14 Mean degree of movement (roll) in response to the stimulus intensity for S1-4. (a) pulse width (PW) = 200, (b) 220, (c) 240 & (d) 260. (note: For S4, data was not collected for PW=200 and I=27.2m

V DISCUSSION

In this work, a biphasic electrical stimulator was designed. A novel feature of this system is the use of an operational amplifier based current source over conventional transformer and MOSFET architectures. The designed system is also programmable and the stimulation current controlled, where the current injected through the electrodes can be precisely controlled by varying the output DAC counts on the micro-controller. The output current therefore, is not effected by the variations in the impedance at the electrode-tissue interface.

Input-output relationship of the device: Figure 11 shows a linear input-output relationship. The sensitivity of the system (0.0068mA/DAC count) is small enough to allow for precise control of the output current as required by FES systems. The sensitivity can be altered if required by adjusting the gains of the difference amplifier. DAC

values between 0-4096 allow for the selection of stimulation amplitude between 0-28mA (experimentally determined value). The difference between the simulated and experimental measured current values increased at larger DAC counts, and as a result, the maximum current measured was 28mA as opposed to the design value of 30mA. In subsequent design iterations, the overall range of the current can be increased if needed without much change to the present hardware framework. The supply rail of the output driving module needs to be boosted, and the resistor Ro in Figure 6 must be decreased to increase the overall current range.

Performance of the device against passive electrical loads: The experimentally measured current values through both the loads showed a high correlation to the simulated values. The error of the output current with respect to the simulated current for load 1 and 2 are -0.976±0.676mA and -0.995±0.97mA, respectively. The error between the loads is low (0.018mA±0.9104mA). From the simulations and experimental data, it is encouraging that the current through the ranges of load (that mimics the human forearm as previously mentioned) is similar, and no considerable variations are seen.

Reduced current range: The drop in the overall range of current amplitude, as previously mentioned, can be attributed to factors such as (a)the tolerance of resistors and resistor mismatch, (b) inaccuracies of the DAC, and (c) op-amp input offset voltage. An obvious solution to mitigate the effect of resistor tolerance is to utilize resistors with lower tolerance but at the price of higher development cost. A trade-off between cost and precision must be considered in subsequent development iterations.

The relation between the degree of stimulated movement and pulse amplitude: The degree of stimulated grasping movement in response to the range of the current pulse amplitude applied in the experiment (19.04mA-27.2mA) varied for the subjects. For all subjects, as the current amplitude increased, the degree of movement also increased. Additionally, a considerable movement was seen for all subjects after 21.76mA except for S4, who showed considerable movement only after 25.84mA. These observations are in accordance with the peak activity - amplitude relationship seen in (23). In this study, it appears that the range of amplitudes applied was in the linear range, and the range of amplitudes where the motion saturates is not entirely tested.

Inter-subject variation in the degree of movement: The inter-subject variations in the degree of movement can be attributed to (a) the effect of body type, subcutaneous tissue(fat) thickness and (b) non optimal placement of electrodes. As mentioned in Section 2.2 currents of high amplitude are required to evoke muscle activation in subjects with thick subcutaneous layers. In our study, S4 has a large BMI (categorized as overweight), and a weak response to the injected current was observed. Inter-subject variation in the degree of movement is also known to depend on electrode positioning. Determining the optimal position of the electrodes for an individual is therefore vital to evoke comparable contractions.

Co-activation of unwanted movements: In this study, a rolling movement was observed about the longitudinal axis of the forearm. The direction of the rolling movement also varied between subjects. The rolling motion is an additional motion observed during the flexion and is not an intended action. The co-activation observed is probably due to the size of the electrodes used in the study. Large-sized electrodes tend to activate neighbouring muscles and bring about unwanted muscle responses. To mitigate this effect, it is possible to reduce the size of the electrode and use multiple smaller target electrodes or use braces to stabilize the motion and prevent motion in unwanted directions. The former solution is more attractive as it provides an opportunity to stimulate more delicate and complex movements

Continuous measurement of stimulated movement: The angles measured using the wrist accelerometer was crucial for obtaining information regarding the flexion movement. The data provided sufficient information regarding the same, and therefore, the location of the sensor was ideal. The motion due to electrical stimulation is a dynamic process dependent on unpredictable factors, as described in Section 2.2. In order to compensate for these factors, the general solution is to introduce currents with large amplitudes to generate magnified and exaggerated muscle response (15). However, this solution induces fatigue and is inefficient. The ability of the device developed in this work to measure angles continuously and in real-time, provides a suitable possibility to develop elegant solutions to adjust the stimulation parameters (like the amplitude, pulse duration and frequency) automatically to an optimal setting.

Limitations and future considerations: In this work, experiments were conducted only on healthy volunteers. Going forward the effectiveness of this system must be clinically validated on subjects with upper limb paralysis. Additionally, testing on a larger sample size of participants will help understand the reason behind the variations observed in response to the stimulation. For future experiments - (a) a more comprehensive range of stimulation parameters must be considered so that relationships between the parameters and the response generated can be understood in detail and determine metrics such as threshold level and saturation level, (b) perform repeated measurements on the same subject to assess variations in successive measurements, (c) take into consideration muscle selectivity to eliminate unwanted contractions, (d) an appropriate method to locate optimal electrode positions, and (e) a design to measure subjective comfort during stimulation.

VI CONCLUSION

In this work, a biphasic, programmable current-controlled functional electrical stimulator system was developed to enable grasping. The system uses an operational amplifier based current source over conventional transformer and MOSFET architectures. The device was validated against two resistive loads and on healthy human participants.

The device can deliver currents between 0-28mA, and the error between the measured current and simulated current for the two passive electrical loads were -0.976±0.676mA and -0.995±0.97mA.

Testing on healthy participants revealed the capability of this device to enable hand grasping. During the experiments, inter-subject variations in the degree of movement and a rolling motion about the longitudinal axis of the forearm was observed. The integration of an accelerometer with this system facilitated the measurement of angular information during the task. The ability of the device to capture angular movement will enable the development of solutions to adjust stimulation parameters automatically to induce movements with desired trajectory. Going forward, we believe that testing the device on patients with upper limb paralysis will provide insights on the clinical effectiveness of the device.

Acknowledgement:

"A part of this work was supported by a BIRAC grant Ref. No. BT/AIR094S/PACE-19/19".

References:

[1] Fakhoury, Marc. "Spinal cord injury: overview of experimental approaches used to restore locomotor activity." Reviews in the Neurosciences 26.4 (2015):397-405.

[2] Béjot, Yannick, Benoît Daubail, and Maurice Giroud. "Epidemiology of stroke and transient ischemic attacks: Current knowledge and perspectives." Revue neurologique 172.1 (2016): 59-68.

[3] Thuret, Sandrine, Lawrence DF Moon, and Fred H. Gage. "Therapeutic interventions after spinal cord injury." Nature Reviews Neuroscience 7.8 (2006): 628-643.

[4] Forrester, Larry W., Lewis A. Wheaton, and Andreas R. Luft. "Exercise-mediated locomotor recovery and lower-limb neuroplasticity after stroke." Journal of Rehabilitation Research Development 45.2 (2008).

[5] Doucet, Barbara M., Amy Lam, and Lisa Griffin. "Neuromuscular electrical stimulation for skeletal muscle function." The Yale journal of biology and medicine 85.2 (2012): 201.

[6] Peckham, P. Hunter, and Jayme S. Knutson. "Functional electrical stimulation for neuromuscular applications." Annu. Rev. Biomed. Eng. 7 (2005): 327-360.

[7] Moreno, Juan C., et al. "Neurorobotic and hybrid management of lower limb motor disorders: a review." Medical biological engineering computing 49.10 (2011): 1119.

[8] Sheffler, Lynne R., and John Chae. "Neuromuscular electrical stimulation in neurorehabilitation." Muscle Nerve: Official Journal of the American Association of Electrodiagnostic Medicine 35.5 (2007): 562-590.

[9] Egglestone, Stefan Rennick, et al. "A design framework for a home-based stroke rehabilitation system: Identifying the key components." 2009 3rd International Conference on Pervasive Computing Technologies for Healthcare. IEEE, 2009.

[10] Cornwell, Andrew S., et al. "A standard set of upper extremity tasks for evaluating rehabilitation interventions for individuals with complete arm paralysis." Journal of rehabilitation research and development 49.3 (2012): 395.

[11] Cheng, KW Eric, et al. "Development of a circuit for functional electrical stimulation." IEEE Transactions on neural systems and rehabilitation engineering 12.1 (2004): 43- 47.

[12] Shendkar, Chandrashekhar, et al. "Design and development of a low-cost biphasic charge-balanced functional electric stimulator and its clinical validation." Healthcare technology letters 2.5 (2015): 129-134.

[13] Jezernik, Saso, Ruben GV Wassink, and Thierry Keller. "Sliding mode closed-loop control of FES controlling the shank movement." IEEE transactions on biomedical engineering 51.2 (2004): 263-272.

[14] Lynch, Cheryl L., and Milos R. Popovic. "Functional electrical stimulation." IEEE control systems magazine 28.2 (2008): 40-50.

[15] Schauer, Thomas. "Sensing motion and muscle activity for feedback control of functional electrical stimulation: Ten years of experience in Berlin." Annual Reviews in Control 44 (2017): 355-374.

[16] Raghavendra, P., et al. "Design and Development of a Real-Time, Low-Cost IMU Based Human Motion Capture System." Computing and Network Sustainability. Springer, Singapore, 2017. 155-165.

[17] Raghavendra, P., et al. "Triggering a Functional Electrical Stimulator Based on Gesture for Stroke-Induced Movement Disorder." Computing and Network Sustainability. Springer, Singapore, 2017. 61-71.

[18] Debur, R., Talasila, V., Sridhar, V., Padmanabh, R., Jayaram, P. and Bhandarkar, A., 2017. Device, System and Apparatus for Functional Electrical Stimulation of Muscle. 10881852.

[19] Sahin, Mesut, and Yanmei Tie. "Non-rectangular waveforms for neural stimulation with practical electrodes." Journal of neural engineering 4.3 (2007): 227.

[20] Marquez-Chin, Cesar, and Milos R. Popovic. "Functional electrical stimulation therapy for restoration of motor function after spinal cord injury and stroke: a review." BioMedical Engineering OnLine 19 (2020): 1-25.

[21] Bhatia, Dinesh, et al. "State of art: functional electrical stimulation (FES)." International Journal of Biomedical Engineering and Technology 5.1 (2011): 77-99.

[22] Lee, Jungeun, Yeongjin Kim, and Hoeryong Jung. "Electrically Elicited Force Response Characteristics of Forearm Extensor Muscles for Electrical Muscle Stimulation-Based Haptic Rendering." Sensors 20.19 (2020): 5669.

[23] Farahat, Waleed, and Hugh Herr. "A method for identification of electrically stimulated muscle."

2005 IEEE Engineering in Medicine and Biology 27th Annual Conference. IEEE, 2006.

[24] Baldwin, Evan RL, Piotr M. Klakowicz, and David F. Collins. "Wide-pulse-width, high-frequency neuromuscular stimulation: implications for functional electrical stimulation." Journal of Applied Physiology 101.1 (2006): 228-240.

[25] Kuhn, Andreas, et al. "A model for transcutaneous current stimulation: simulations and experiments." Medical biological engineering computing 47.3 (2009): 279-289.

[26] Department of Biochemistry and Molecular Biophysics Thomas Jessell, Steven Siegelbaum, and A. J. Hudspeth. Principles of neural science. Eds. Eric R. Kandel, James H. Schwartz, and Thomas M. Jessell. Vol. 4. New York: McGraw-hill, 2000.

[27] Gorman, Peter H., and J. Thomas Mortimer. "The effect of stimulus parameters on the recruitment characteristics of direct nerve stimulation." IEEE Transactions on Biomedical Engineering 7 (1983): 407-414.

[28] Merrill, Daniel R., Marom Bikson, and John GR Jefferys. "Electrical stimulation of excitable tissue: design of efficacious and safe protocols." Journal of neuroscience methods 141.2 (2005): 171-198.

[29] Kumsa, Doe, et al. "Electrical neurostimulation with imbalanced waveform mitigates dissolution of platinum electrodes." Journal of neural engineering 13.5 (2016): 054001.

[30] O'Dwyer, S. B., et al. "An electrode configuration technique using an electrode matrix arrangement for FES-based upper arm rehabilitation systems." Medical engineering physics 28.2 (2006): 166-176.

[31] Malešević, Nebojša M., et al. "A multi-pad electrode based functional electrical stimulation system for restoration of grasp." Journal of neuroengineering and rehabilitation 9.1 (2012): 1-12.

[32] "Education," Axelgaard Education Wrist and Finger Flexion. [Online]. Available: https://www.axelgaard.com/Education/Wrist-and-Finger-Flexion. [Accessed: 03- Feb-2021]

[33] Button, Vera. Principles of Measurement and transduction of biomedical variables. Academic Press, 2015.

[34] Keller, Thierry, and Andreas Kuhn. "Electrodes for transcutaneous (surface) electrical stimulation." Journal of Automatic Control 18.2 (2008): 35-45.

[35] Luna, José Luis Vargas, et al. "Dynamic impedance model of the skin-electrode interface for transcutaneous electrical stimulation." PloS one 10.5 (2015): e0125609.

[36] Shimada, Yoichi, et al. "Clinical use of percutaneous intramuscular electrodes for functional electrical stimulation." Archives of physical medicine and rehabilitation 77.10 (1996): 1014-1018.

[37] Doheny, Emer P., et al. "Effect of subcutaneous fat thickness and surface electrode configuration during neuromuscular electrical stimulation." Medical engineering physics 32.5 (2010): 468-474.

[38] Badger, James, Paul Taylor, and Ian Swain. "The safety of electrical stimulation in patients with pacemakers and implantable cardioverter defibrillators: A systematic review." Journal of Rehabilitation and Assistive Technologies Engineering 4 (2017): 2055668317745498.

[39] Maundy, Brent J., Ahmed S. Elwakil, and Stephan JG Gift. "Enhancing the improved Howland circuit." International Journal of Circuit Theory and Applications 47.4 (2019): 532-541.

[40] Pease, Robert A. "AN-1515 a comprehensive study of the Howland current pump." Dallas: Texas Instruments (2013): 1-17.

[41] Anand, G., A. Lowe, and A. M. Al-Jumaily. "Parametric electrical modelling of human forearm simulation response using multi-frequency electrical bioimpedance." Journal of Biosensors Bioelectronics 7 (2016).

[42] Gholami-Boroujeny, Shiva, and Miodrag Bolic. "Extraction of Cole parameters from the electrical bioimpedance spectrum using stochastic optimization algorithms." Medical biological engineering computing 54.4 (2016): 643-65

[43] Sandra Marquez-Figueroa, Yuriy S. Shmaliy, Oscar Ibarra-Manzano, "Improving Gaussianity of EMG Envelope for Myoelectric Robot Arm Control", WSEAS Transactions on Biology and Biomedicine, vol. 18, pp. 106-112, 2021.

[44] Sandra Marquez-Figueroa, Yuriy S. Shmaliy, Oscar Ibarra-Manzano, "Improving Gaussianity of EMG Envelope for Myoelectric Robot Arm Control", WSEAS Transactions on Biology and Biomedicine ,vol 18, pp 106-112,2021.